

Widespread Deregulation of Phosphorylation-Based Signaling Pathways in Multiple Myeloma Cells: Opportunities for Therapeutic Intervention

Gwenny Manel Fuhler,^{1*} Sander Henricus Diks,^{2*} Maikel Petrus Peppelenbosch,^{1†} and William Garrow Kerr^{3†}

¹Department of Gastroenterology and Hepatology, Erasmus MC, University Medical Center Rotterdam, Rotterdam, the Netherlands;

²Department of Cell Biology, Section of Immunology, University Medical Center Groningen, Hanzeplein, Groningen, the Netherlands;

³Departments of Pediatrics and Microbiology & Immunology, SUNY Upstate Medical University, Syracuse, New York, United States of America

Multiple myeloma (MM) is a neoplasm of plasma cell origin that is largely confined to the bone marrow (BM). Chromosomal translocations and other genetic events are known to contribute to deregulation of signaling pathways that lead to transformation of plasma cells and progression to malignancy. However, the tumor stroma may also provide trophic support and enhance resistance to therapy. Phosphorylation of proteins on tyrosine, serine and threonine residues plays a pivotal role in cell growth and survival. Therefore, knowing the status of phosphorylation-based signaling pathways in cells may provide key insights into how cell growth and survival is promoted in tumor cells. To provide a more comprehensive molecular analysis of signaling disruptions in MM, we conducted a kinome profile comparison of normal plasma cells and MM plasma cells as well as their surrounding cells from normal BM and diseased BM. Integrated pathway analysis of the profiles obtained reveals deregulation of multiple signaling pathways in MM cells but also in surrounding bone marrow blood cells compared to their normal counterparts. The deregulated kinase activities identified herein, which include the mTOR (mammalian target of rapamycin)/p70S6K and ERK1/2 (extracellular signal-regulated kinases 1 and 2) pathways, are potential novel molecular targets in this lethal disease.

© 2011 The Feinstein Institute for Medical Research, www.feinsteininstitute.org

Online address: <http://www.molmed.org>

doi: 10.2119/molmed.2011.00013

INTRODUCTION

Multiple myeloma (MM) is a plasma cell (PC) neoplasm that leads to renal failure, hypercalcemia and skeletal destruction resulting in a median length of survival at diagnosis of approximately 3–5 years (1). There are thought to be three general categories of factors that promote the growth and/or survival of MM cells *in vivo* (2,3). The first consists of factors such as interleukin 6 (IL-6), IL-10 and interferon- α that trigger JAK/STAT (janus kinase/signal transducer and activator of transcription) pathways, which can lead to activation

of mitogen-activated protein (MAP) kinases that drive cell proliferation. In addition, insulinlike growth factor (IGF)-1, HGF (hepatocyte growth factor) and EGF (epidermal growth factor) family members that engage syndecan-1 are known to activate not only proliferative pathways via the MAP kinases, but also survival pathways via activation of the phosphatidylinositol 3-kinase (PI3K)/Akt/mammalian target of rapamycin (mTOR) pathway. The third pathway involves the B-lineage-specific BAFF (B-cell activating factor) and April receptors, whose ligands can trigger activa-

tion of PI3K/Akt and nuclear factor κ -light-chain-enhancer of activated B cells (NF- κ B) activities that promote cell survival.

High-throughput analysis systems have defined the transcriptome and proteome of MM and other tumor cells (4–6). Novel insights in the MM transcriptome have led to the notion that the majority of transcripts are necessary to keep a cell functioning and could be regarded as the minimal transcriptome. Only a small portion of the transcripts present in the cell determine the identity of the cell, and these critical transcripts are normally expressed at low levels. Therefore small changes in the expression profiles in this part of the transcriptome can lead to large changes in the enzymatic profile of the cell, leading to significant differences in cell functioning (7). Hence, an equally, if not more important, goal is to define the activity of the proteins that control the status of signal-

*GMF and SHD are equal contribution first authors for this paper.

†MPP and WGK are equal contribution last authors for this paper.

Address correspondence and reprint requests to William G Kerr, WH2204, 750 E. Adams Street, SUNY Upstate Medical University, Syracuse, NY 13210. Phone: 315-464-5850; Fax: 315-464-4417; E-mail: kerrw@upstate.edu.

Submitted January 10, 2011; Accepted for publication April 26, 2011; Epub (www.molmed.org) ahead of print April 28, 2011.

ing pathways available in experimental models (8). Kinases, the enzymes that phosphorylate tyrosine, serine and threonine residues on other proteins, play a major role in controlling the status of signaling cascades that determine, for example, cell cycle entry and survival. Knowing the status of signaling pathways in MM cells and their supporting stroma could provide critical information for understanding MM cell survival in the bone marrow (BM). Thus, a comprehensive description of cellular metabolism could be a valuable complement to descriptions of the proteome and transcriptome. We have developed a novel array-based strategy that allows the simultaneous detection of enzymatic activities for the phosphorylation of different kinase substrates in one cell sample (9–11). Here we apply this technology to primary MM isolates to assess the differences in kinase activity between MM cells and their normal PC counterparts, in addition to stromal elements that may also have an impact on MM growth and survival. These large-scale kinome comparisons reveal multiple, deregulated signaling pathways in MM and the surrounding BM blood cells and reveal potential novel avenues for therapy in this deadly blood cell cancer.

MATERIALS AND METHODS

Patient Samples

For cell sorting, MM primary patient samples were obtained from the liquid tissue acquisition core at H. Lee Moffitt Cancer Center. Mononuclear cells were collected by the tissue acquisition staff via Ficoll-gradient centrifugation. For normal PC sorts and phosphoflow, normal human BM samples were received as mononuclear cell suspensions in Hanks' balanced salt solution with 5 mmol/L EDTA and 0.5% bovine serum albumin (1M-125; Lonza-Poietics, Basel, Switzerland). For phosphoflow analysis, non-MM and MM samples were obtained from the Frozen Liquids Tissue Core at H. Lee Moffitt Cancer Center.

Fluorescence-Activated Cell Sorting

The populations of interest were sorted from both the MM and the normal human BM mononuclear cells in the same manner. The Fc receptors were blocked with anti-human CD32, and the sample was stained with anti-human CD38–fluorescein isothiocyanate (FITC), anti-human CD138–phycoerythrin (PE) and DAPI (4'6-diamidino-2-phenylindole-2HCl). The CD38^{hi}CD138⁺ and CD38[−]CD138[−] populations were collected separately by use of fluorescence-activated cell sorting (FACS) with an FACS Aria (BD, Franklin Lakes, NJ, USA).

FACS Analysis

Cell surface marker expression on non-PC was analyzed by staining BM mononuclear cell fractions with the following antibodies: CD45-FITC, CD19-FITC, CD34-FITC, CD3-FITC, CD41a-APC, CD14-FITC, CD71-FITC, CD33-FITC, CD138-FITC, CD11b-FITC, CD36-FITC, VCAM-FITC (CD106) or glycoporphin A (GPA)-PE. To exclude PC and dead cells, samples were simultaneously stained for CD38-PE or CD38-FITC and DAPI.

Phosphoflow

The phosphoflow monoclonal antibody anti-ERK1/2(pT202/pY204), conjugated to Alexa Fluor 647, was purchased from BD Pharmingen (San Diego, CA, USA). Cells were stained with CD38, CD138 and p-ERK, or the appropriate isotype control according to the manufacturer's protocol for phosphoflow analysis of human peripheral blood mononuclear cells.

Determination of the Phosphoproteome

Each of the MM or normal BM (NBM) isolates prepared were applied to a PepChip slide. The PepChip used for profiling is the kinase v1 version containing duplicates of 1176 spots (1152 plus 24 control spots) derived from the annotated PhosphoBase (version 2.0) (57). Information on phosphorylation sites can be obtained through <http://www.hprd.org/>.

For the array samples, 0.5×10^6 cells were lysed in cell lysis buffer (20 mmol/L Tris-HCl, pH 7.5, 150 mmol/L NaCl, 1 mmol/L Na₂EDTA, 1 mmol/L EGTA, 1% Triton X-100, 2.5 mmol/L sodium pyrophosphate, 1 mmol/L MgCl₂, 1 mmol/L beta-glycerophosphate, 1 mmol/L Na₃VO₄, 1 mmol/L NaF, 1 µg/mL leupeptin, 1 µg/mL aprotinin, 1 mmol/L phenylmethylsulfonyl fluoride), and debris was removed by centrifugation. The peptide array incubation mix was produced by adding 10 µL of filter-cleared activation mix (50% glycerol, 50 µmol/L ATP, 0.05% v/v Brij-35, 0.25 mg/mL bovine serum albumin) and 2 µL [γ -³³P] ATP (approximately 1000 kBq; Amersham AH9968, Amersham Biosciences, Piscataway, NJ, USA). Next, the peptide array mix was added onto the chip, and the chip was kept at 37°C in a humidified incubator for 90 min. Subsequently the peptide array was washed twice with Tris-buffered saline with Tween 20, twice in 2 mol/L NaCl, and twice in demineralized H₂O, and then air-dried. The chips were exposed to a phosphoimager plate for 72 h, and the density of the spots was measured and analyzed with array software (ScanAnalyze).

Data Analysis

The 5% and 95% intervals of the spot density were calculated for each data set, and all spots were normalized within the boundaries for which the 5% level equals 0 and 95% is given the value 100. If only background phosphorylation is present, this amplitude-based distribution can be described by a single exponent. Because at low intensities of phosphorylation the contribution of biological phosphorylation is minimal, and hence the data in this range contain almost exclusively pure noise, we determined the exponent describing the amplitude behavior of the 250 least phosphorylated peptides, ranked from lowest to highest intensities, to give an adequate description of array background phosphorylation. True phosphorylation events were considered to have occurred for peptides of which the average phosphorylation minus z times the

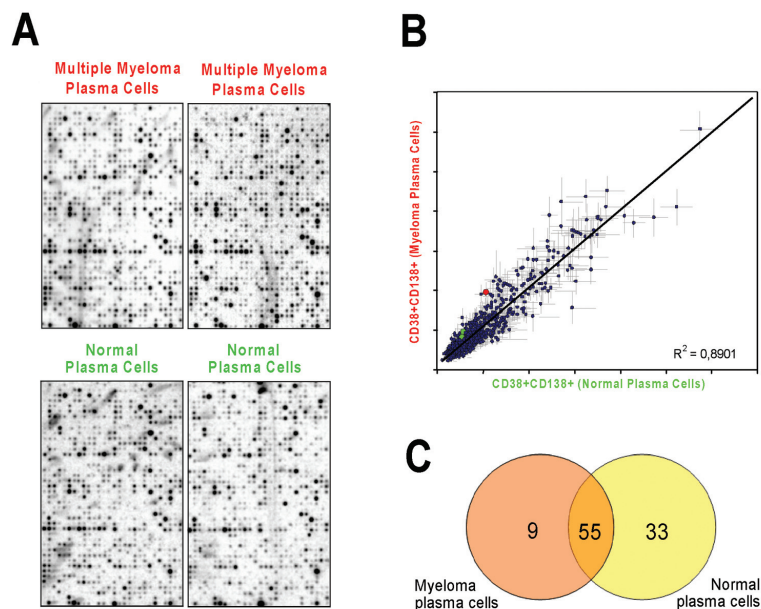


Figure 1. Comparison of the MM cell and normal PC phosphoproteomes. (A) Phosphoimager scans of “1152” spot PepChip™ for MM cells (red) and normal PC (green) from two representative MM patients and two normal donors. (B) Scatter plot showing the mean amount of phosphorylation detected by PepChip™ for all 1152 substrates in MM cells (y axis) versus normal PC (x axis). Each spot on the plot represents the mean phosphorylation across 10 different MM cell sorts (y axis) and 10 different normal PC sorts (x axis). Indicated in the graph are the differently phosphorylated substrates Insulin receptor signaling (green) and S6 Kinase (red). (C) Venn diagram of number of substrates receiving an “on” call according to Markov analysis of the mean substrate phosphorylation of lysates from 10 MM patients and 10 normal donors.

SD was higher than the value expected from describing the background distribution. For integrated pathway analysis, z was a floating value designed to maximize difference between the kinomes; for all other analyses z was set to 1.96, which yielded a P value of 0.05 or better for each “on” call made. The set of peptides that thus showed statistically significant phosphorylation compared to the background was then subjected to elective Markov analysis, i.e., assuming that different peptides acting as substrates for the same kinase have different affinity for phosphorylation by this kinase, kinases more active in one condition compared to another condition should display in the more active condition more phosphorylated target peptides. Thus the extent to which a kinase activity can be determined precisely is dependent on the number of substrates for the kinase (hence analysis

for epidermal growth factor receptor (EGFR), for which only 2 peptides are present on the chip, is much more imprecise than analysis for protein kinase B, for which >15 peptides are present).

Western Blot Analysis

Sorted cells were lysed in cell lysis buffer as described above. Protein concentration was determined by bicinchoninic acid protein assay (Pierce, Rockford, IL, USA) according to the manufacturer’s instructions. Laemmli sample buffer was added to the samples and sodium dodecyl sulfate–polyacrylamide gel electrophoresis (SDS–PAGE) and immunoblotting were performed as described (58). Detection was performed according to the manufacturer’s guidelines (ECL, Pierce, Rockford, IL, USA). All phosphoantibodies were from Cell Signaling Technology (Beverly, MA, USA).

Membranes were reprobed with an antibody against actin (Santa Cruz Biotechnology, Santa Cruz, CA, USA), and densitometry of the blots was performed using ImageMaster 1D Elite (Pharmacia, Woerden, the Netherlands).

Cell Viability Assay

MM cell lines RPMI8226, U266 and OPM2 were routinely maintained in RPMI1640 (PAA Laboratories, Etobicoke, Ontario, Canada) supplemented with 10% fetal calf serum (PAA Laboratories). Cells were treated in duplicate for 36 h with increasing concentrations of sirolimus (LC Laboratories, Woburn, MA, USA), U1026 (Cell Signaling Technology) or protein kinase G (PKG) inhibitor (Calbiochem, Merck, Darmstadt, Germany). 3-(4,5-Dimethylthiazol-2-yl)-2,5-diphenyltetrazolium bromide (MTT) (Sigma, St Louis, MO, USA) was added at a concentration of 0.5 mg/mL to the cells for 3 h. Formed crystals were dissolved in dimethyl sulfoxide and optical density (OD) was measured at 570 nm. The OD of compound treated cells was divided by the OD of their vehicle control, and the viability was expressed as a percentage of untreated cells. Results are expressed as mean \pm SEM of three individual experiments.

All supplementary materials are available online at www.molmed.org

RESULTS

Comparison of MM and NBM PC Kinome

MM cells present in BM can be identified by the expression of high levels of CD38 and CD138 (12). CD38^{hi}CD138⁺ MM cells from BM aspirates were obtained from 10 different patients and 10 different healthy BM donors with NBM (see representative Bone Marrow Sort, Supplementary Figure 1). We subsequently conducted a comparison of the kinase activities present in MM cells to those present in normal PC by applying PepChip array technology on the isolates. Figure 1A shows representative

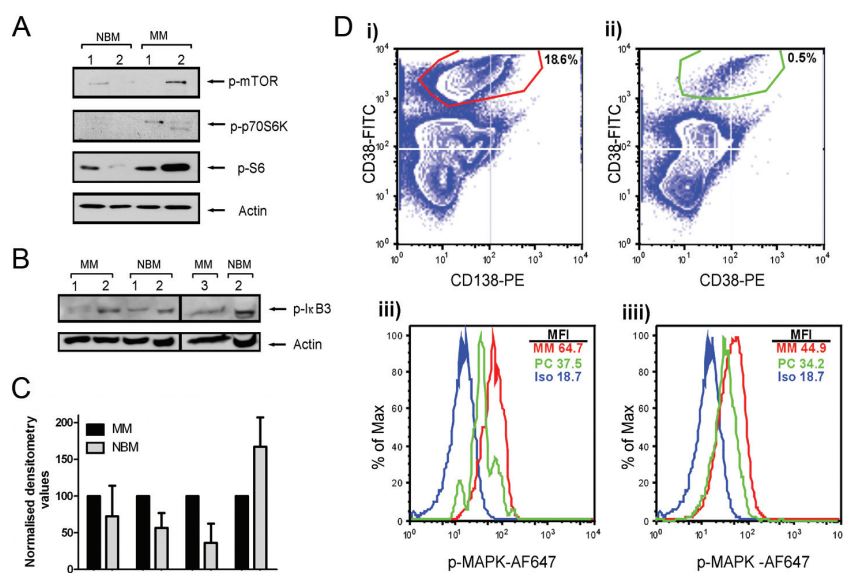


Figure 2. Validation of PepChip analysis of MM and normal PC sorts. (A,B) Sorted CD38^{hi} CD138⁺ cells from MM patients or NBM donors were lysed and proteins were separated by SDS-PAGE, after which the blots were probed with antibodies against phosphorylated mTOR, p70S6K and S6 ribosomal protein (A) or phosphorylated I κ B (B). Equal loading was confirmed by reprobing the blots with antibodies against actin. (C) For quantification of phosphorylated protein, densitometry values were divided by the densitometry values of total actin protein present in the same samples. The values obtained for NBM patient samples are represented as a percentage of densitometry values of MM samples. Mean \pm SEM of data are shown. (D) (i) Gating strategy to identify MM cells in a representative MM patient BM aspirate. MM cells were identified by the CD38^{hi}CD138⁺ phenotype (red polygon). (ii) Gating strategy to identify normal PC in a non-MM BM aspirate (green polygon). (iii, iiiii) Two individual experiments in which phospho-MAPK levels in CD38^{hi}CD138⁺ MM plasma cells (red histogram) or CD38^{hi}CD138⁺ normal PC (green histogram) and isotype-matched control stains for CD38^{hi}CD138⁺ cells present in pooled MM and non-MM BM aspirates (blue histogram). The mean fluorescence intensity (MFI) for the p-MAPK stains and the isotype control stain are indicated in the upper right hand corner of each pairwise comparison of CD38^{hi}CD138⁺ cells in MM and non-MM BM.

PepChip phosphorimager scans for purified MM and NBM PC from 2 of 10 different MM patients and 2 of 10 normal donors. In Figure 1B we show an MM *versus* a normal PC profile scatter plot in which each dot represents the normalized mean phosphorylation level for each of the 1152 substrates arrayed in duplicate on the PepChip for all MM cell and normal PC samples analyzed. As expected there is a great deal of similarity between the two kinomes; however, there is also a distinct subset of substrates that fall off the diagonal. Among these are the p70S6K target ribosomal protein S6 and the insulin receptor, the phosphorylation of which was increased

in MM PC (Figure 1B). The insulin receptor shares 60% homology with the IGF-1 receptor, and binding of IGF-1 leads to its autophosphorylation and activation. IGF-receptor signaling is one of the most important growth, survival and migration signals for MM PC, and numerous groups have reported autocrine IGF-1 production for primary MM cells and myeloma cell lines (13,14).

Characterization of the Deregulated Kinome in MM Plasma Cells

Next, the normalized values were subjected to Markov analysis, which resulted in the generation of an “on” or “off” call for each kinase substrate, much

like what is generally done for gene expression profiling, representing phosphorylation events that were significantly above background. To obtain a first insight into the characteristics of the PC kinome in general and the differences between the PC kinome and the MM kinome in particular, we performed an integrated pathway analysis using a floating value of z (see Materials and Methods) to maximize the contrast between the two datasets. The results are presented in Supplementary Figure 2, which depicts for the two cell types for different kinases the fraction of kinase substrates receiving an “on” call. These results show that the differences between the two kinomes are mainly localized to the activation of the mTOR signaling pathway and the MAP kinase pathway. Subsequently, we fixed z to yield a P value of 0.05 for each “on” call, which diminishes contrast between the kinomes but provides good confidence in statements made. In total, 64 kinase substrates received an “on” call in MM PC versus 88 in NBM PC, with an overlap of 55 spots (see Supplemental Table S1 and Figure 1C). The nine significantly phosphorylated substrates that are specific for MM PC include cGMP-dependent protein kinase (PKG), cAMP response-binding element (CREB), histone H2A, histone 1A and myosin light chain 2.

Upregulation of the mTOR-p70S6K-S6 and ERK1/2 Pathways in MM PC

In MM but not NBM PC, PepChip data showed significant phosphorylation of the Ser133 target sequence of CREB, a known substrate for S6K and the MAPK ERK1/2, suggesting an enhanced constitutive activity of these pathways in MM cells. To validate this in a method independent of PepChip analysis, we sorted CD38^{hi}CD138⁺ cells from two new MM patients and healthy donors, and compared the phosphorylation (and hence activation) status of the major molecules in this pathway according to Western blot analysis. Figures 2A and C show that phosphorylation levels of mTOR, p70S6K and S6 ribosomal protein, al-

though variable, as a mean were higher in MM PC compared with those in their normal counterparts.

To validate increased MAPK pathway activity in MM cells, we examined the level of MAPK phosphorylation in primary MM cells and normal PC by PhosphoFlow (Figure 2D). This analysis showed increased phosphorylation, and hence activity, of MAPK in MM cells compared with normal PC in both pairs of BM aspirates analyzed (Figure 2D, *i,iii* and *ii,iii*), consistent with our PepChip findings.

Next, we performed functional analysis of the dependence of MM cells on mTOR and MEK-ERK pathways for survival. Inhibition of either of these pathways with a selective inhibitor (i.e., sirolimus and U0126, respectively) decreases numbers of viable cells in three MM cell lines (Figure 3A, B). The data shown in Figure 3D demonstrate that treatment of MM cells with sirolimus inhibits constitutive and IGF-induced phosphorylation of both p70S6k and S6, but not ERK1/2. Vice versa, U0126 inhibits ERK1/2 phosphorylation, but not that of the p70S6k-S6 pathway. Interestingly, combined treatment at concentrations that induce very little cell death individually inhibited phosphorylation of both the P70S6K-S6 and ERK1/2 pathways, resulting in an additive effect on cell viability (Figure 3C). These data corroborate the notion that simultaneous inhibition of two independent survival pathways (i.e., p70S6K and ERK1/2) may be beneficial in the treatment of MM.

Phosphoproteome of Normal PC

The substrates that received an “on” call in NBM PC, but not in MM PC, included IL-1 α , as well as the Src kinase substrate focal adhesion kinase (FAK), which activates the phosphorylation site Tyr577, and Annexin II. In light of the fact that PC from high-risk MM patients have been described to express high levels of IL-1 β , this may seem surprising. IL-1 is thought to stimulate para- and autocrine IL-6 production in MM (15,16), and is a known physiological activator of

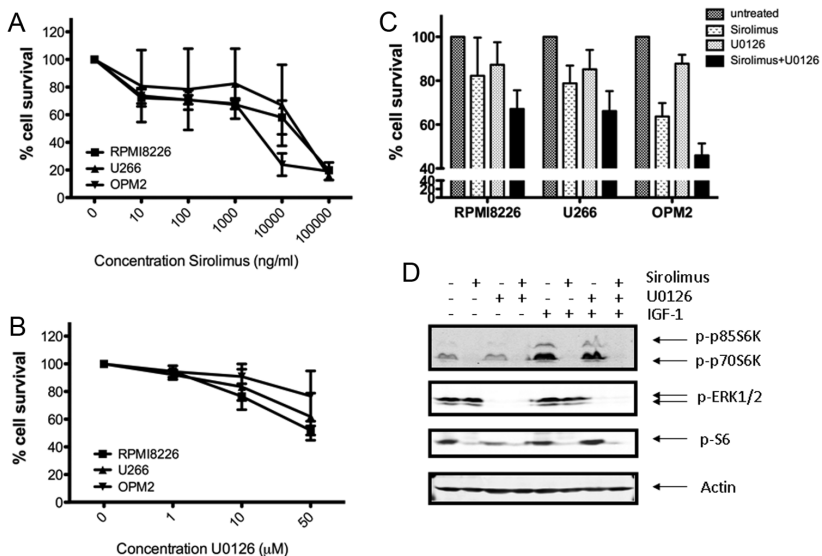


Figure 3. Additive cell killing by ERK and mTOR pathway inhibitors in MM cells. (A, B) MM cell lines were treated for 48 h with increasing concentrations of sirolimus or U0126, after which viable cell number was determined by MTT. Mean of 3 independent experiments is shown. (C) MM cell lines were treated with 100 μ mol/L sirolimus, 10 μ mol/L U0126 or a combination thereof. MTT assay was performed in three independent experiments and results represent the mean percentage survival rate of cells. (D) MM cells were treated with 100 μ mol/L sirolimus (2 h), 10 μ mol/L U0126 (30 min) or a combination thereof, after which cells were lysed and proteins were separated by SDS-PAGE. Blots were probed with antibodies against phosphorylated p70S6K, S6 ribosomal protein and ERK1/2. Equal loading was confirmed by reprobing the blots with antibodies against actin.

NF- κ B in B-lymphoid cells (17). Activation of NF- κ B through FAK has been reported to play a role in IL-6 production in myoblasts (18). In addition, Src activity has been linked to NF- κ B activity in mediating B-cell development (19). Activation of NF- κ B requires its release from inhibitory factors, inhibitors of κ B (I κ Bs), which are degraded upon phosphorylation by I κ B kinases. We used Western blot analysis to compare I κ B phosphorylation in three MM patients with that in two healthy controls, and we observed variable phosphorylation of I κ B, with a higher mean densitometry in normal PC, suggestive of NF- κ B activation (Figure 3B, C).

Comparison of MM and NBM Non-PC Kinomes

MM PC are known to influence their BM microenvironment directly, by cytokine production and stimulation of osteoclast activity, and indirectly, by physi-

cal reduction of BM space by MM PC accumulation, resulting in impaired residual hematopoiesis. Indeed, by FACS analysis we observed significantly lower percentages of T cells (CD3 $^{+}$), early myeloid cells (CD33 $^{+}$) and granulocytic cells (CD11b $^{+}$) in MM BM (n = 7) compared to normal BM (n = 6) (Supplementary Figure 3).

To determine whether there are significant signaling differences between the MM and normal BM microenvironment cells, we also sorted non-PC from 10 MM patients and 10 NBM donors (See Supplementary Figure 1 for an example of sorting and Figure 4A for representative PepChip phosphorimager scans). This fraction is enriched for cells from the erythroid lineage (CD36 $^{+}$, CD71 $^{+}$, GPA $^{+}$) (Supplemental Figure 3B). Figure 4B shows a MM versus normal non-PC phosphoproteome profile scatter plot, indicating a high degree of similarity between these groups. Markov analysis re-

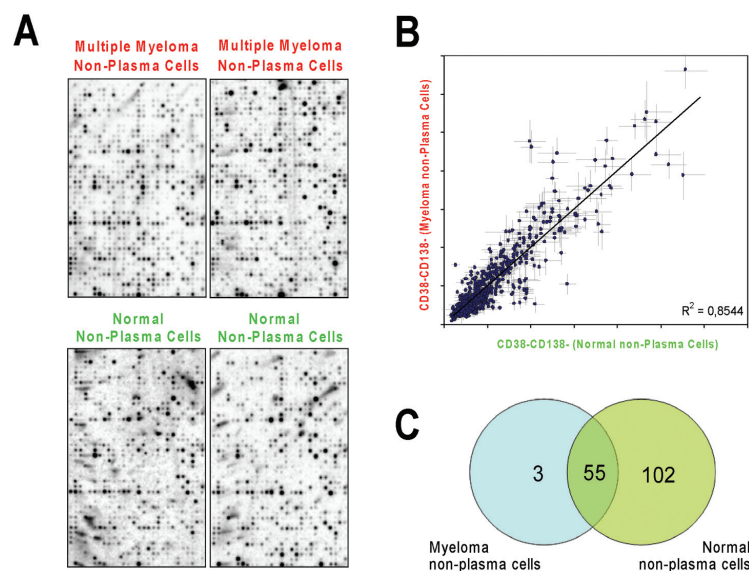


Figure 4. Comparison of the microenvironment phosphoproteomes in MM BM and NBM. (A) Representative phosphoimager scans of “1152” spot PepChip™ for CD38⁻CD138⁻ stroma cells from two different NBM donors (green) and two different MM BM patients as indicated (red). (B) Scatter plot showing the mean level of phosphorylation for all 1152 substrates in MM CD38⁻CD138⁻ cells (y axis) versus normal BM CD38⁻CD138⁻ cells (x axis). Each spot on the plot represents the mean phosphorylation across 10 different MM cell sorts (y axis) and 10 different normal PC sorts (x axis). (C) Venn diagram of number of substrates receiving an “on” call according to Markov analysis of the mean substrate phosphorylation of 10 MM patient and 10 normal donor non-PC lysates.

sulted in an “on” call for 58 kinase substrates in MM non-PC, compared to 102 in NBM samples, with an overlap of 55 substrates (Supplemental Table S2). An “on” call was present for five vimentin-specific substrates in NBM CD38⁻CD138⁻ cells, which were not present in MM stromal cells, a result that is strongly suggestive of a more adhesive phenotype in normal stromal cells. Vimentin is phosphorylated by active PAK2 kinase, and an increased phosphorylation (and hence activation) of PAK2 in CD38⁻CD138⁻ cell lysates from two individual MM patients and two healthy BM donors was confirmed by Western blot analysis (Figure 5).

Whereas in PC, S6K and ERK signaling were increased in MM samples, the opposite was observed in non-PC samples. Two substrates for ERK1/2 kinase activity and one for 6S-kinase were phosphorylated in NBM cells, but not MM samples. In addition, phosphorylation of eukaryotic translation and initiation fac-

tor 4F, a target of the mTOR/p70S6K pathway, was also observed in normal CD38⁻CD138⁻ cells. Western blotting indeed showed an increased phosphorylation of mTOR, p70S6K and S6 in normal stromal elements compared with MM non-PC, a finding indicative of activation of this pathway.

These results suggest widespread downregulation in signaling in MM BM cells, although the mixture of cell types present makes it impossible to assign kinase activity to individual populations and speculate on the meaning for these cell types. However, these results do demonstrate that in addition to MM PC, non-PC BM cells in general are also deregulated in MM patients.

Common Targets in MM Plasma Cells and MM Stromal Cells

In a final step we checked whether there are common substrates that are affected in both PC and stromal cells in MM. Correlation analysis of mean phos-

phorylation of substrates shows a high correlation between MM PC and NBM PC (0.92), and between MM non-PC and NBM non-PC (0.903). However, this high degree of correlation was not observed when PC and non-PC were compared in MM patients (0.77) or NBM (0.79), suggesting that PC have a kinome profile that is distinct from the rest of the BM. Per donor, correlations ranged from 0.667 to 0.89 for MM patients (mean 0.78 ± 0.072) and from 0.53 to 0.96 for NBM donors (mean 0.80 ± 0.14). No overlap was found between the substrates that received an “on” call in MM PC but not normal PC and those that were “on” in MM non-PC versus NBM non-PC. In contrast, of the 33 spots more strongly phosphorylated in NBM CD38^{hi}CD138⁺ PC compared with MM PC, 25 (76%) were also upregulated in NBM CD38⁻CD138⁻ non-PC compared with MM non-PC, indicating common deregulation of these pathways in both tumor and microenvironmental cells in MM BM. However, whereas 33 kinase targets were more phosphorylated in NBM PC, 102 spots were specifically upregulated in non-PC from healthy controls compared with their MM counterparts. This large difference might be the result of the presence of multiple individual cell types in the CD38⁻CD138⁻ fraction, all contributing to the overall kinome profile. Of 189 target sequences phosphorylated in all four groups, i.e., PC and non-PC from MM and NBM, 43 received an “on” call in all of these. These sequences and the kinases they represent are likely the minimal kinome that is active in BM-derived cells.

DISCUSSION

We used the PepChip platform to determine which signaling pathways are deregulated in MM by directly comparing purified cell populations prepared from MM and normal BM isolates. We successfully demonstrated that the phosphoproteome of MM cells is significantly different from that of their normal PC counterparts.

In MM PC, 64 kinase substrates were phosphorylated versus 88 in normal PC.

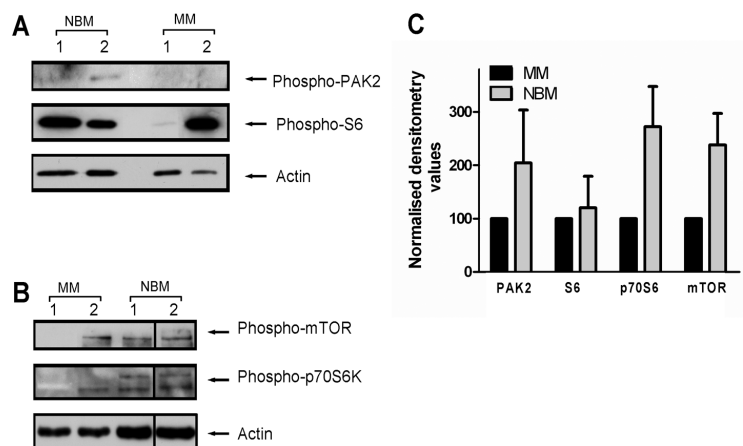


Figure 5. Validation of PepChip analysis of MM and normal non-PC sorts. (A, B) Sorted CD38⁺CD138⁻ non-PC from MM patients or normal donors (NBM) were lysed and proteins were separated by SDS-PAGE, after which the blots were probed with antibodies against phosphorylated FAK, PAK2 and S6 ribosomal protein (A) or phosphorylated mTOR or p70S6K (B). Equal loading was confirmed by reprobing the blots with antibodies against actin. (C) For quantification of phosphorylated protein, densitometry values were divided by the densitometry values of total actin protein present in the same samples. Results are subsequently presented as percentage of corrected MM densitometry values.

In non-PC, 58 kinase substrates received an “on” call in MM samples compared with 157 in NBM. These numbers demonstrate that kinase activity in general is dramatically decreased in diseased cells compared with normal cells. This result is somewhat surprising, because many studies have focused on inhibition of active signaling pathways as a strategy for treatment of this disease. However, most studies have focused either on stimulated kinase activity or on constitutive activity as a secondary result of another defect, such as deletion of the phosphatases PTEN (phosphatase and tensin homolog) or CD45 (20,21), which is not very common in MM (22). Our results suggest that although some pathways are highly constitutively activated in MM cells, the remaining kinome profile is repressed, a finding that may well reveal fundamental aspects of the transformed cells; the focus it has on proliferative pathways can result in a downregulation of other pathway activities, which are normally important in untransformed cells. In other words, the amount of energy available to a transformed cell may be redistributed to lead to overactivation

of relatively few pathways, at a cost of other cellular signaling pathways. Similar results were demonstrated in acute myeloid leukemia (AML) cells, suggesting that this phenomenon might be common in hematological malignancies (A ter Elst, personal communication).

One of the phosphorylated substrates in MM PC was PKG, which has been best described regarding its role in mediating nitric oxide (NO) signaling (23). Hypoxic factors such as NO are capable inducers of angiogenesis, and NO signaling through PKG has been linked to insulin-induced production of vascular endothelial growth factor (VEGF-1) in smooth muscle cells (24). This potent angiogenic factor is also secreted by MM cells in response to IGF-1 stimulation, and increased VEGF-1 serum levels are correlated with poor prognosis in MM patients (25,26). Interestingly, malignant MM PC express high levels of nitrotyrosine, a marker of NO presence, and NO-synthase 1, 2 and 3. In addition, serum levels of NO are elevated in MM patients (27,28). Interestingly, orally tolerable NO-synthase inhibitors are available, and were shown to have antiangiogenic ef-

fects in a MM mouse model, reducing both tumor burden and VEGF production by MM cells (29). In addition to a role in angiogenesis, NO-activated PKG has also been implicated in antiapoptotic mechanisms in leukemic cells (30). We now show that chemical inhibition of PKG indeed reduces cell viability in three different MM cell lines (Supplementary Figure 4). Therefore, it is interesting to speculate on a potential benefit of NO-synthase or PKG inhibitors in the treatment of MM.

Our data showed an “on” call for FAK, Src kinase and IL-1 α in normal PC, but not MM PC, in conjunction with an increased phosphorylation of I κ B phosphorylation, suggestive of NF- κ B activity. However, several studies have shown that NF- κ B activation is present in MM cells. Inhibitors of this pathway, such as the proteasome inhibitor Bortezomib, which inhibits NF- κ B activity by preventing degradation of I κ B, have been shown to be of clinical benefit in 35% of patients (31). Our results might be explained by the fact that MM can be a heterogeneous disease, and in our analysis we show only substrates that were as a mean activated in 10 individual donors. In other words, although individual MM patients might present with increased NF- κ B activity, this might not show up in a cross-examination of 10 patients. Furthermore, proteasome inhibitors are most effective when used in cotreatment strategies (32,33). Recently it was reported that NF- κ B activity in MM cells was enhanced by conventional drugs like melphalan and doxorubicin, and was subsequently inhibited by proteasome inhibitors like Bortezomib (34). Because our MM samples were obtained at diagnosis, this might explain why we do not find an enhanced I κ B phosphorylation in these patients.

Our analysis of the deregulated substrates in MM PC showed increased MAPK and mTOR/p70S6K pathway activity. These changes, in combination with other mutations, might be sufficient to cause the MM cell to assume malignant properties. Alternatively, early re-

ports suggested that apoptosis induction in MM cells in response to therapeutic agents like dexamethasone was a result of downregulation by these agents of the MAPK and p70S6K pathways (35). Later studies indicated that inhibition of mTOR by rapamycin-sensitized MM cell lines and primary MM cells to dexamethasone treatment (36), which was also shown in an *in vivo* mouse model (37). Our study results showing increased (constitutive) phosphorylation of the mTOR-p70S6K-S6 pathway in primary MM PC, and the sensitivity of MM cells to sirolimus, provide a rationale and incentive for the use of mTOR inhibitors in the treatment of MM. Interestingly, phase I/II clinical trials are currently being performed with NVP-BEZ235, an orally bioavailable compound that has been shown to reduce mTOR activity and MM proliferation (38). However, in addition to mTOR, this drug also targets the PI3K pathway. Given that our PepChip analysis did not reveal a major deregulation of this pathway in an average of 10 MM patients, more specific inhibitors, targeting only mTOR and its downstream components, might be more beneficial owing to reduced off-target effects. In fact, such inhibitors, e.g., rapamycin and its analogues RAD001 and sirolimus, were found to be orally tolerated in a range of studies targeting solid tumors. Recently however, phase I clinical trials of temsirolimus have been initiated in cotreatment regimens for MM that involve dexamethasone, Bortezomib or Lenalidomide (39). Based on our data, the use of mTOR inhibitors might be further enhanced by cotreatment with specific ERK1/2 inhibitors. An oral small molecule MEK/ERK inhibitor, AZD6244, has entered phase I/II clinical trials in patients with solid tumors, and, based on our results, may be beneficial in MM patients (40).

We propose that therapeutic approaches to treat MM could use two different regimens. One regimen employs inhibitors against multiple targets in MM PC (for example, MAPK and mTOR), or uses an approach in which deregulated

kinases in both MM cells and their stroma are targeted. With the second approach deregulated growth of MM cells is counteracted via direct inhibition and through a less favorable environment (poisoning both the seed and soil to eradicate tumor cells). In conclusion, our findings show that phosphoproteome determination is a valuable tool to generate a global view of kinases deregulated in MM and to provide putative targets for treatment.

DISCLOSURE

The authors declare that they have no competing interests as defined by *Molecular Medicine*, or other interests that might be perceived to influence the results and discussion reported in this paper.

REFERENCES

- Kyle RA, Rajkumar SV. (2004) Multiple myeloma. *N. Engl. J. Med.* 351:1860–73.
- Klein B, et al. (2003) Survival and proliferation factors of normal and malignant plasma cells. *Int. J. Hematol.* 78:106–13.
- Hwang JJ, Ghobrial IM, Anderson KC. (2006) New frontiers in the treatment of multiple myeloma. *ScientificWorldJournal.* 6:1475–1503.
- Zhan F, et al. (2006) The molecular classification of multiple myeloma. *Blood.* 108:2020–28.
- Wurmbach E, et al. (2002) Validated genomic approach to study differentially expressed genes in complex tissues. *Neurochem. Res.* 27:1027–33.
- Tarte K, et al. (2004) The Bcl-2 family member Bfl-1/A1 is strongly repressed in normal and malignant plasma cells but is a potent anti-apoptotic factor for myeloma cells. *Br. J. Haematol.* 125:373–82.
- Hanahan D, Weinberg RA. (2000) The hallmarks of cancer. *Cell.* 100:57–70.
- Parikh K, Peppelenbosch MP, Ritsema T. (2009) Kinome profiling using peptide arrays in eukaryotic cells. *Methods Mol. Biol.* 527:269–80.
- van Baal JW, et al. (2006) Comparison of kinome profiles of Barrett's esophagus with normal squamous esophagus and normal gastric cardia. *Cancer Res.* 66:11605–12.
- de Borst MH, et al. (2006) Profiling of the renal kinome: A novel tool to identify protein kinases involved in angiotensin II-dependent hypertensive renal damage. *Am. J. Physiol. Renal. Physiol.* 293:F428–37.
- Lowenberg M, et al. (2006) Kinome analysis reveals nongenomic glucocorticoid receptor-dependent inhibition of insulin signaling. *Endocrinology.* 147:3555–62.
- Lin P, Owens R, Tricot G, Wilson CS. (2004) Flow cytometric immunophenotypic analysis of 306 cases of multiple myeloma. *Am. J. Clin. Pathol.* 121:482–88.
- Sprynski AC, et al. (2009) The role of IGF-1 as a major growth factor for myeloma cell lines and the prognostic relevance of the expression of its receptor. *Blood.* 113:4614–26.
- Menu E, Van VE, Van CB, Vanderkerken K. (2009) The role of the insulin-like growth factor 1 receptor axis in multiple myeloma. *Arch. Physiol. Biochem.* 115:49–57.
- Lust JA, et al. (2009) Induction of a chronic disease state in patients with smoldering or indolent multiple myeloma by targeting interleukin 1[β]-induced interleukin 6 production and the myeloma proliferative component. *Mayo Clin. Proc.* 84:114–22.
- Xiong Y, et al. (2006) Identification of two groups of smoldering multiple myeloma patients who are either high or low producers of interleukin-1. *J. Interferon. Cytokine Res.* 26:83–95.
- Bomsztyk K, et al. (1991) Evidence that interleukin-1 and phorbol esters activate NF-kappa B by different pathways: role of protein kinase C. *Cell. Regul.* 2:329–35.
- Tseng WP, Su CM, Tang CH. (2010) FAK activation is required for TNF-alpha-induced IL-6 production in myoblasts. *J. Cell. Physiol.* 223:389–96.
- Saijo K, et al. (2003) Essential role of Src-family protein tyrosine kinases in NF-kappaB activation during B cell development. *Nat. Immunol.* 4:274–79.
- Descamps G, et al. (2004) The magnitude of Akt/phosphatidylinositol 3'-kinase proliferating signaling is related to CD45 expression in human myeloma cells. *J. Immunol.* 173:4953–59.
- Zhang J, Choi Y, Mavromatis B, Lichtenstein A, Li W. (2003) Preferential killing of PTEN-null myelomas by PI3K inhibitors through Akt pathway. *Oncogene.* 22:6289–95.
- Chang H, et al. (2006) Analysis of PTEN deletions and mutations in multiple myeloma. *Leuk. Res.* 30:262–65.
- Wang X, Robinson PJ. (1997) Cyclic GMP-dependent protein kinase and cellular signaling in the nervous system. *J. Neurochem.* 68:443–56.
- Eleutherakis-Papaiakovou V, Karali M, Kokkonouzis I, Tiliakos I, Dimopoulos MA. (2003) Bone marrow angiogenesis and progression in multiple myeloma: clinical significance and therapeutic approach. *Leuk. Lymphoma.* 44:937–48.
- Doronzo G, et al. (2004) Insulin activates vascular endothelial growth factor in vascular smooth muscle cells: influence of nitric oxide and of insulin resistance. *Eur. J. Clin. Invest.* 34:664–73.
- Pour L, et al. (2009) Levels of angiogenic factors in patients with multiple myeloma correlate with treatment response. *Ann. Hematol.* 89:385–9.
- Mendes RV, Martins AR, de NG, Murad F, Soares FA. (2001) Expression of nitric oxide synthase isoforms and nitrotyrosine immunoreactivity by B-cell non-Hodgkin's lymphomas and multiple myeloma. *Histopathology.* 39:172–8.

28. Kuku I, *et al.* (2005) Oxidant/antioxidant parameters and their relationship with medical treatment in multiple myeloma. *Cell. Biochem. Funct.* 23:47–50.
29. Uneda S, *et al.* (2003) A nitric oxide synthase inhibitor, N(G)-nitro-L-arginine-methyl-ester, exerts potent antiangiogenic effects on plasmacytoma in a newly established multiple myeloma severe combined immunodeficient mouse model. *Br. J. Haematol.* 120:396–404.
30. Kolb JP. (2000) Mechanisms involved in the pro- and anti-apoptotic role of NO in human leukemia. *Leukemia.* 14:1685–94.
31. Richardson PG, Mitsiades C, Ghobrial I, Anderson K. (2006) Beyond single-agent bortezomib: combination regimens in relapsed multiple myeloma. *Curr. Opin. Oncol.* 18:598–608.
32. Min CK, *et al.* (2007) Bortezomib in combination with conventional chemotherapeutic agents for multiple myeloma compared with bortezomib alone. *Jpn. J. Clin. Oncol.* 37:961–8.
33. Curran MP, McKeage K. (2009) Bortezomib: a review of its use in patients with multiple myeloma. *Drugs.* 69:859–88.
34. Baumann P, Mandl-Weber S, Oduncu F, Schmidmaier R. (2008) Alkylating agents induce activation of NFkappaB in multiple myeloma cells. *Leuk. Res.* 32:1144–7.
35. Chauhan D, *et al.* (1997) Dexamethasone induces apoptosis of multiple myeloma cells in a JNK/SAP kinase independent mechanism. *Oncogene.* 15:837–43.
36. Stromberg T, *et al.* (2004) Rapamycin sensitizes multiple myeloma cells to apoptosis induced by dexamethasone. *Blood.* 103:3138–47.
37. Yan H, *et al.* (2006) Mechanism by which mammalian target of rapamycin inhibitors sensitize multiple myeloma cells to dexamethasone-induced apoptosis. *Cancer Res.* 66:2305–13.
38. Baumann P, Mandl-Weber S, Oduncu F, Schmidmaier R. (2009) The novel orally bioavailable inhibitor of phosphoinositol-3-kinase and mammalian target of rapamycin, NVP-BEZ235, inhibits growth and proliferation in multiple myeloma. *Exp. Cell Res.* 315:485–97.
39. Dancey JE, Curiel R, Purvis J. (2009) Evaluating temsirolimus activity in multiple tumors: a review of clinical trials. *Semin. Oncol.* 36(Suppl 3):S46–58.
40. Adjei AA, *et al.* (2008) Phase I pharmacokinetic and pharmacodynamic study of the oral, small-molecule mitogen-activated protein kinase kinase 1/2 inhibitor AZD6244 (ARRY-142886) in patients with advanced cancers. *J. Clin. Oncol.* 26:2139–46.